^{13}C NMR Spectroscopic and X-ray Crystallographic Study of the Role Played by Mitochondrial Cytochrome b_5 Heme Propionates in the Electrostatic Binding to Cytochrome c[†,‡]

María J. Rodríguez-Marañón,[§] Feng Qiu,[||] Ruth E. Stark,[||] Steven P. White,[⊥] Xuejun Zhang,[£] Stephen I. Foundling,[£] Verónica Rodríguez,[§] Curtis L. Schilling, III,[§] Richard A. Bunce,[§] and Mario Rivera*[,§]

Department of Chemistry, Oklahoma State University, Stillwater, Oklahoma 74078, Department of Biochemistry and Molecular Biology, Oklahoma State University, Stillwater, Oklahoma 74078, Crystallography Program, Oklahoma Medical Research Foundation, 825 NE 13th Street, Oklahoma City, Oklahoma 73104, and Department of Chemistry, College of Staten Island, City University of New York, Staten Island, New York 10314

Received July 31, 1996; Revised Manuscript Received October 23, 1996[⊗]

ABSTRACT: The role played by the outer mitochondrial membrane (OM) cytochrome b_5 heme propionate groups in the electrostatic binding between OM cytochrome b_5 and horse heart cytochrome *c* was investigated by ^{13}C NMR spectroscopy and X-ray crystallography. To achieve these aims, ^{13}C-labeled heme OM cytochrome b_5 was expressed in *Escherichia coli* as previously described [Rivera M., Walker, F. A. (1995) *Anal. Biochem. 230*, 295−302]. Assignment of the resonances arising from the heme propionate carbons in ferricytochrome b_5 was carried out by a combination of one- and two-dimensional NMR experiments. Titrations of [^{13}C]heme-labeled OM cytochrome b_5 with horse heart cytochrome *c* were carried out in order to monitor the resonances arising from the heme propionate carbonyl carbons in OM cytochrome b_5. The results from these titrations clearly show that only the heme propionate located on the exposed heme edge in OM cytochrome b_5 participates in the electrostatic stabilization of the complex between OM cytochrome b_5 and horse heart cytochrome *c*. Similar experiments carried out monitoring ^{13}C resonances arising from several other heme substituents demonstrated that the stoichiometry of the complex is 1:1. A conditional binding constant, *K* which equals $3.8 \times 10^4 \pm 1.4 \times 10^4$ at $\mu = 0.02$ M, was obtained for the formation of the complex by fitting the binding curves obtained experimentally to a model based on this stoichiometry. The X-ray crystal structure of rat liver OM cytochrome b_5 solved to 2.7 Å resolution shows that the structures of bovine liver microsomal cytochrome b_5 and rat liver OM cytochrome b_5 are almost identical when compared at medium resolution. The similarity between the two structures, combined with the findings that only the heme propionate located on the exposed heme edge of OM cytochrome b_5 participates in the electrostatic binding to cytochrome *c* and that the stability of this complex is similar to that measured for the association between microsomal cytochrome b_5 and cytochrome *c*, clearly indicates that the site of interaction on OM cytochrome b_5 is almost identical to the one elucidated for microsomal cytochrome b_5. It is therefore possible to conclude that the large body of information gathered by many investigators for the nonphysiological interaction between microsomal cytochrome b_5 and cytochrome *c* (recently reviewed) [Mauk, A. G., Mauk, M. R., Moore, G. R., & Northrup, S. H. (1995) *Bioenerg. Biomembr. 27*, 311−330] has indeed biological as well as pedagogical validity.

It is widely accepted that the formation of interprotein complexes precedes most interprotein electron transfer reactions. The first interprotein complex of this kind for which a model was postulated is the one that leads to the reduction of ferricytochrome *c* by ferrocytochrome b_5 (Salemme, 1976). The hypothetical model of the complex was based on the known three-dimensional structures of bovine liver microsomal cytochrome b_5 and horse heart cytochrome *c*, and it assumed that the stability of the complex was provided by electrostatic interaction between acidic residues on the surface of cytochrome b_5 and basic residues on the surface of cytochrome *c*. These acidic and basic residues are asymmetrically distributed on the surface of these cytochromes, thus generating a large concentration of charged residues in close proximity to the heme active site of both proteins. The model proposed by Salemme (1976) stimulated the development of experimental strategies aimed at studying the cytochrome b_5−cytochrome *c* complex which has become a paradigm for the investigation of similar complexes formed by electron transfer proteins. The interaction domain of microsomal cytochrome b_5 with cytochrome *c* was mapped using site-directed mutagenesis and hyperbaric pressure spectroscopy (Rodgers *et al.*, 1988; Sligar *et al.*, 1991), and it was concluded that the region of interaction on the surface of cytochrome b_5 encompasses the area that

[†] The financial support of NIH Grants GM 50503 and AHA 9507904S to M.R. are gratefully acknowledged. The NMR facilities, operated by the CUNY Center for Applied Biomedicine and Biotechnology and the College of Staten Island, were provided by a grant from the National Science Foundation (BIR-9214560 to R.E.S.) and by the City University of New York.

[‡] Coordinates have been deposited in the Brookhaven Protein Data Bank (file name 1b5m).

* To whom correspondence should be addressed.

[§] Department of Chemistry, Oklahoma State University.

[||] City University of New York.

[⊥] Department of Biochemistry and Molecular Biology, Oklahoma State University.

[£] Oklahoma Medical Research Foundation.

[⊗] Abstract published in *Advance ACS Abstracts,* December 1, 1996.

S0006-2960(96)01895-8 CCC: $12.00

surrounds the exposed heme edge in cytochrome b_5. Two recent reviews (Mauk *et al.*, 1995; Durham *et al.*, 1995) summarize the multidisciplinary effort undertaken by several investigators which has resulted in the development of a variety of experimental strategies aimed at studying the association of these two proteins in aqueous solution.

The large majority of studies reported to date have been carried out with the water soluble domain of microsomal cytochrome b_5 and horse heart cytochrome *c*. It is noteworthy that the heme binding domain and the domain used to anchor cytochrome b_5 to the membrane are known to be independent of each other, with the heme binding domain retaining full activity after tryptic digestion aimed at separating this domain from the membrane binding domain (Strittmatter & Ozols, 1966). It is also important to recognize that, due to cellular compartmentalization, the likelihood of interaction between microsomal cytochrome b_5 and cytochrome *c*, which is normally associated with the mitochondrial interprotein space, is low. The 58% sequence homology between mitochondrial and microsomal isoforms of cytochrome b_5 (Lederer *et al.*, 1983; Rivera *et al.*, 1992), however, indicates that the interactions between microsomal cytochrome b_5 and cytochrome *c* may be a good representation of the interactions between the mitochondrial cytochromes b_5 and c.

Mitochondrial cytochrome b_5 was isolated and purified from the outer membranes of mitochondria by proteolytic cleavage (Fukushima & Sato, 1972) and by detergent solubilization (Nisimoto *et al.*, 1977). The proteolytically cleaved rat liver outer mitochondrial membrane (OM) cytochrome b_5 was purified and proved to be distinct from the microsomal cytochrome b_5 isolated from rat liver (Ito, 1980) and later shown to be 58% homologous to microsomal cytochrome b_5 (Lederer *et al.*, 1983). It has been shown that mitochondrial cytochrome b_5 participates in the rotenone-insensitive transfer of electrons from NADH to cytochrome *c* oxidase via cytochrome *c* (Bernardi & Azzone, 1981) and that the aerobic oxidation of exogenous NADH by mitochondria involves a pathway in which electrons flow from NADH to NADH cytochrome b_5 reductase, which in turn reduces OM cytochrome b_5 in the outer mitochondrial membrane. OM cytochrome b_5 subsequently reduces cytochrome *c* which shuttles the electron across the intermembrane space in order to reduce cytochrome *c* oxidase in the inner mitochondrial membrane. A form of NADH dehydrogenase having the same stereochemical properties with respect to NADH and capable of reducing OM cytochrome b_5 has been found in the outer mitochondrial membrane. Whether this enzyme is identical to microsomal cytochrome b_5 reductase is not yet known (Raw *et al.*, 1960; Sottocasa *et al.*, 1967).

A gene coding for the water soluble domain of rat hepatic OM cytochrome b_5 has been synthesized and expressed in *Escherichia coli* (Rivera *et al.*, 1992), and although the UV−vis, EPR, and ^{1}H NMR spectra of the overexpressed mitochondrial protein were shown to be almost identical to the spectra exhibited by the microsomal isoform, the reduction potential of mitochondrial cytochrome b_5 is −102 mV *vs* NHE (Rivera *et al.*, 1994). By comparison, the reduction potential of trypsin-cleaved bovine liver microsomal cytochrome b_5 is 5.1 mV (Reid *et al.*, 1982) or −1.9 mV (Walker *et al.*, 1988). It is therefore relevant to ask if the interactions between mitochondrial cytochrome b_5 and cytochrome *c* are indeed very similar to those observed between microsomal cytochrome b_5 and cytochrome *c*. In order to answer this question, we have utilized a recently developed technique which allows selective isotopic labeling of the heme in cytochrome b_5 (Rivera & Walker, 1995) in order to carry out ^{13}C NMR spectroscopic studies aimed at elucidating the role played by the OM cytochrome b_5 heme propionates in the electrostatic binding of this protein to cytochrome *c*. These studies show that only the heme propionate which is on the exposed heme edge of OM cytochrome b_5 participates in electrostatic binding to cytochrome *c*, thus indicating that the area of interaction on the surface of mitochondrial cytochrome b_5 also includes the exposed heme edge. Furthermore, the interpretation of the NMR data was corroborated by obtaining the X-ray crystal structure of OM cytochrome b_5, which clearly shows that the structures of rat liver OM cytochrome b_5 and bovine liver microsomal cytochrome b_5 are indeed very similar.

EXPERIMENTAL PROCEDURES

Crystal Growth and X-ray Crystallography Data Collection. X-ray quality crystals of OM cytochrome b_5 were grown using the vapor diffusion method utilizing the 50 buffer Crystal Screen from Hampton Research. The protein was dissolved in deionized water to a concentration of 20 mg/mL and mixed with each buffer in a hanging drop. Crystals were obtained by vapor diffusion together with slow evaporation using 20% PEG 8000 in 0.1 M sodium cacodylate (pH 6.5) with 0.2 M magnesium acetate. The crystal of rat outer mitochondrial membrane cytochrome b_5 used in data collection belongs to the Laue group *P*4/*mmm* with the following unit cell parameters: $a = b = 30.0$ Å and $c = 219.0$ Å. X-ray data were collected to 2.7 Å resolution using a Siemens multiwire area detector. Following integration and data reduction, the total number of reflections used for the final structural refinement was 3123 with an R_{symm} of 0.045. The data completeness was 96% in the 2.7−20.0 Å shell and 91% in the 2.7−2.8 Å shell.

Biosynthesis of ^{13}C-Labeled Heme Cytochrome b_5. ^{13}C-labeled 5-aminolevulinic acid (ALA) was used to prepare the ^{13}C-labeled hemes incorporated into cytochrome b_5. Details of the synthesis of these labeled precursors are reported elsewhere (Kajiwara *et al.*, 1989; Bunce, R. A., *et al.*, manuscript in preparation). OM cytochrome b_5 labeled with ^{13}C at the heme active site was obtained by a modification of the method reported by Rivera and Walker (1995). A single colony of BL21(DE3) *E. coli* cells previously tranformed with the recombinant plasmid MRL2 (Rivera *et al.*, 1992) was used to inoculate 5 mL of LB medium containing 100 μg/mL ampicillin and allowed to grow until the OD_{600} was 2.0, approximately 8 h. This culture (100 μL) was used to inoculate 50 mL of M9 minimal medium (Sambrook *et al.*, 1989) supplemented with the following salts: ammonium sulfate (0.1%), nitriloacetate (1 mM), magnesium sulfate (20 mM), calcium chloride (0.45 μM), ammonium molybdate(VI) (0.15 μM), ferrous sulfate (40 μM), EDTA (17 μM), copper(II) sulfate (3 μM), cobalt(II) nitrate (2 μM), zinc sulfate (7.6 μM), and sodium borate (9.4 μM) (Stanier & Palleroni, 1966). The 50 mL culture was diluted to 1 L with fresh medium and allowed to grow to an OD_{600} of 1 (4−6 h) before polypeptide biosynthesis was induced by addition of IPTG to a final concentration of

1 mM. Ten minutes after the addition of IPTG, biosynthesis of heme was induced by addition of 17 mg of ^{13}C-labeled 5-aminolevulinic acid and 71 mg of $FeCl_2$ per liter of culture. Purification to homogeneity of the overexpressed [^{13}C]heme-labeled cytochrome was carried out as described by Rivera and Walker (1995).

NMR Spectroscopy. Titrations monitored by ^{13}C NMR were carried out with a Varian XL 400 spectrometer operating at a ^{13}C frequency of 100.6 MHz. Typically, OM cytochrome b_5 solutions (1−2 mM) were prepared in 5 mM perdeuterated phosphate buffer at pH 7.0 (not corrected for the isotope effect). OM cytochrome b_5 used in the titration experiments was exhaustively dialyzed against water, exchanged with D_2O, and subsequently freeze-dried. Cytochrome *c* was purchased from Sigma and was extensively dialyzed against water, freeze-dried, and subsequently used to prepare a 15 mM solution in 5 mM perdeuterated phosphate buffer at pH 7.0. Protein concentrations were determined spectrophotometrically utilizing an ϵ_{412} of 130 mM^{-1} cm^{-1} for OM ferricytochrome b_5 (Bodman *et al.*, 1986) and an ϵ_{416} of 109.1 mM^{-1} cm^{-1} for ferricytochrome *c* (Margoliash & Walasek, 1967). Titration of ferricytochrome b_5 with ferricytochrome *c* was performed by adding a solution of cytochrome *c* to a solution containing OM cytochrome b_5. Titrations monitored with resonances arising from heme α-propionate and α-vinyl carbons were carried out at 30 °C with a spectral width of 35 kHz, 21K data points, a 300 ms acquisition time, and no relaxation delay. Typically, 12000−14000 scans were acquired for every point in the titration. Titrations monitored with resonances arising from the heme propionate carbonyl carbons were acquired at 30 °C with a spectral width of 9.5 kHz, 21K data points, a 1.1 s acquisition time, and a 200 ms relaxation delay. Typically, 5000−7000 scans were acquired for each point in the titration curve. Titrations monitored with resonances attributed to isomer A 5−methyl and isomer B 8-methyl were acquired at 30 °C with a spectral width of 35 kHz, 30K data points, a 0.4 s acquisition time, and a 500 ms relaxation delay. Typically, 3000−8000 scans were acquired for each point in the titration curve.

Resonance assignments were carried out with a Varian *Unityplus* 600 spectrometer operating at ^{1}H and ^{13}C frequencies of 599.95 and 150.87 MHz, respectively. For heterocorrelated single-quantum coherence (HSQC) experiments, a pulsed-field gradient method (Kay *et al.*, 1992; Ouwen *et al.*, 1994) was used to minimize artifacts. The two-dimensional spectrum was acquired with spectral widths of 36 kHz for ^{1}H and 60 kHz for ^{13}C, respectively, a $^1J_{CH}$ set to 140 Hz, a relaxation delay of 0.4 s, and WURST decoupling on the ^{13}C channel (Kupce & Freeman, 1995). The data were collected as an array of 4K × 1K points, which after linear prediction in the t_1 dimension and zero filling in both dimensions produced a 4K × 4K data matrix. For heterocorrelated multiple-bond coherence (HMBC) experiments, Varian's ghmqc pulse sequence was used with *z*-axis-pulsed field gradients. The acquisition conditions were similar to those used for HSQC, but 2K × 1K data points were acquired and $^2J_{CH}$ was set to 14 Hz (instead of the more customary 9 Hz) in order to shorten the interpulse delays and minimize signal losses due to the short T_2 of the heme resonances. The ^{1}H−^{13}C−^{13}C filtered ^{1}H experiment was carried out using a ^{13}C−^{13}C double-quantum filter and ^{1}H detection (Qiu, F., *et al.*, manuscript in preparation). The parameters included 32 000 data points spanning a ^{1}H spectral width of 36 kHz, a $^1J_{CH}$ set to 140 Hz, and a $^1J_{CC}$ set to 45 Hz. The relaxation delay was set to 1.0 s, and WURST decoupling was applied on the ^{13}C channel. Finally, ^{13}C spectra were obtained with ^{13}C continuous-wave homonuclear decoupling, using a field strength of 4.7 kHz and beginning 0.2 s before acquisition. The relaxation delay was set to 0.7 s; no ^{1}H broad band decoupling was applied in these latter experiments. The resulting spectra had 36K data points over a ^{13}C spectral width of 60 kHz.

RESULTS

Crystallographic Molecular Replacement Solution. Given the Laue group *P*4/*mmm* of the crystal, there is one cytochrome b_5 protein molecule per crystallographic asymmetric unit with a V_M of 2.2 Å^3/Da (Matthews, 1968). The initial phases for the crystal structure of OM cytochrome b_5 were solved using molecular replacement methods (Rossmann, 1972). Since the amino acid sequence of OM cytochrome b_5 is 58% identical (53 out of 87 residues) with that of bovine liver microsomal cytochrome b_5, the coordinates corresponding to the crystal structure of the latter, which was refined using 1.5 Å X-ray diffraction data (Durley & Mathews, 1996), was used as the search model for the molecular replacement calculation which was carried out with the computer program package MRCHK (Zhang & Matthews, 1994).

X-ray diffraction data in the range of 3.6−8.0 Å were used for the calculation of both the rotation function and the translation function. The search for a molecular replacement solution was straightforward in spite of the search model containing 35 amino acid residues which are different from those found in OM cytochrome b_5. The rotation function solution was 1.3 standard deviations (SD) above the top noise peak. Furthermore, the translation function search confirmed the rotation function solution and demonstrated that the space group of the mitochondrial cytochrome b_5 crystal is $P4_32_12$. A translation function solution stood out from the noise by 2.0 SD. The corresponding model had an initial crystallographic *R* factor of 0.48 (3.5−20.0 Å) and good crystal packing.

Refinement. The refinement of the crystal structure of rat liver OM cytochrome b_5 was carried out using the molecular refinement program package TNT (Tronrud *et al.*, 1987). A rigid body refinement using 3.5−20.0 Å diffraction data reduced the *R* factor from 0.48 to 0.41. Subsequent cycles of model building using the graphic program O (Jones *et al.*, 1991) and individual coordinate refinement with fixed thermal factors was carried out with 3.0−20.0 Å data, and the *R* factor was reduced to 0.32. Further refinement using 2.7−20.0 Å data and correlated thermal factor restraints (Tronrud, 1996) resulted in a model with an *R* factor of 0.22 and good geometry. The statistics of the refinement are summarized in Table 1.

In spite of the overall structural similarity between the structures of rat liver OM cytochrome b_5 and beef liver microsomal cytochrome b_5, the local conformations at both the amino and the carboxy termini in the two crystal structures are significantly different from each other. This difference reflects the different length of the two protein molecules at their carboxy termini, different packing environments in the two crystal forms, as well as substitutions

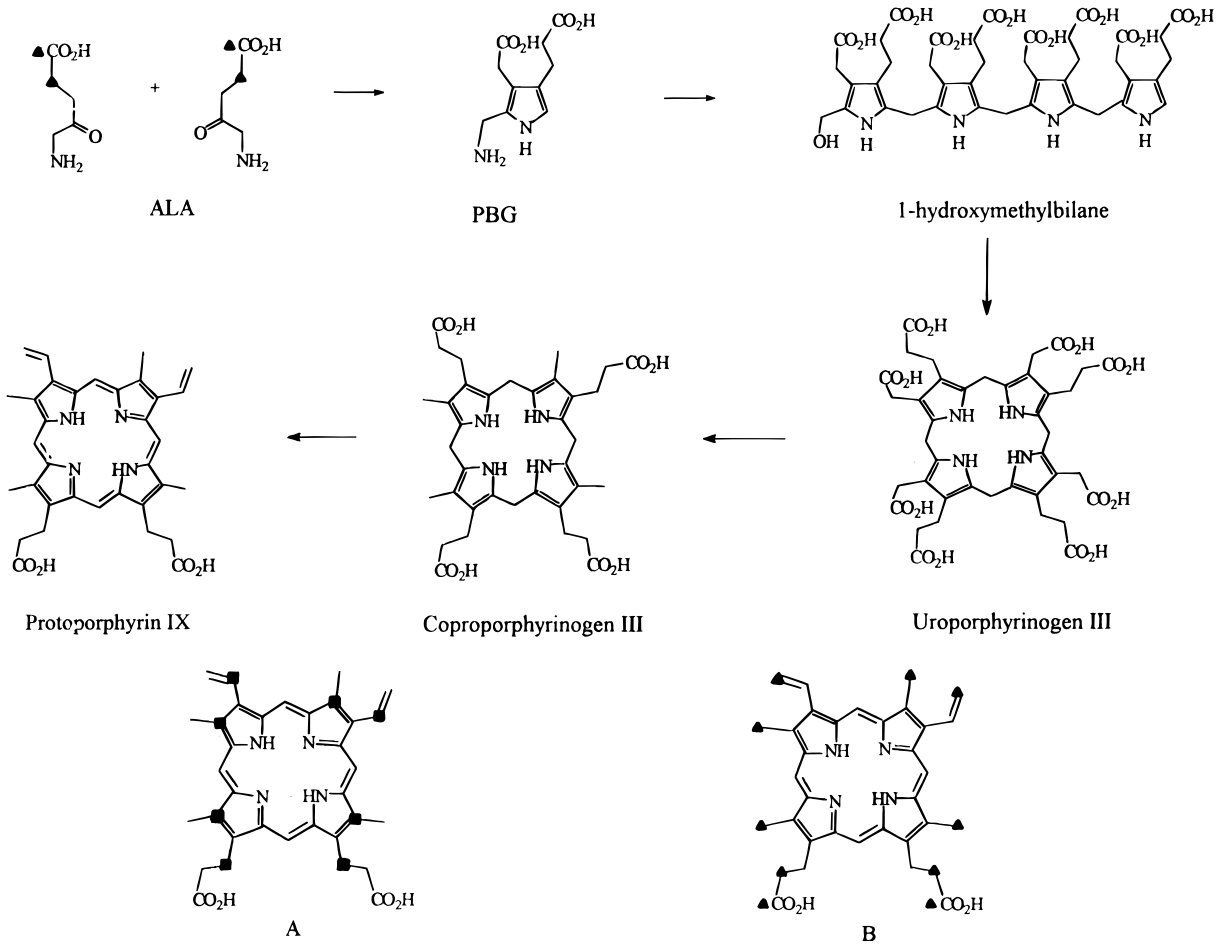

FIGURE 1: Schematic representation of the heme biosynthetic pathway in which δ-aminolevulinic acid is the first committed precursor. The introduction of iron into protoporphyrin IX, which is catalyzed by ferrochelatase, is not shown in the scheme. When [3-^{13}C]-δ-ALA is used as a heme precursor, heme labeled at positions denoted by ■ in structure A is obtained. When [1,2-^{13}C]-δ-ALA is used as a heme precursor, heme labeled at positions denoted by ▲ in structure B is obtained.

Table 1: Statistics of the Final Model as Refined by TNT[a]

resolution range (Å)	2.7−20.0
number of reflections used for refinement	3123
number of non-hydrogen atoms	719
average *B* factor (Å^2)	
protein backbone	36
heme	31
rmsd	
bond (Å)	0.016
angle (deg)	3.0
R factor	0.22

[a] *R* factor = $||F_o| - |F_c||/|F_o|$. rmsd = root mean square deviation.

in their amino acid sequences. Residues at both ends of mitochondrial cytochrome b_5 were omitted in the initial model and were gradually added to the model at later stages of the refinement as the phases improved. Since electron density at the very ends of both termini is not well defined, residues 1, 2, and 87 were not included in the final refined model of the crystal structure of mitochondrial cytochrome b_5.

The heme group in cytochrome b_5 is found in two possible orientations which are related to each other by a 180° rotation about the α,γ-meso axis. During the refinement, attempts were made to determine the orientation(s) of the heme group in the crystal structure of mitochondrial cytochrome b_5. At the given 2.7 Å resolution, the electron density of the heme group slightly favors the predominant orientation observed in the crystal structure of microsomal cytochrome b_5, and this orientation was used in the final refined model of mitochondrial cytochrome b_5. Given the medium resolution of the X-ray diffraction data, no solvent molecules were explicitly included in the current model of the refined crystal structure. Multiple conformations were not included for either amino acid residues or heme group substituents in the refined model.

^{13}C NMR Assignments. It has been previously demonstrated that, when isotopically labeled ALA is used as a precursor of heme biosynthesis, isotopically labeled heme is obtained in relatively high yields, provided that the concentration of free heme in *E. coli* is kept relatively low. This has been achieved by simultaneously overexpressing apocytochrome b_5, whose function is to sequester the relatively large amounts of heme that are made by the cell upon addition of ALA to the culture media (Rivera & Walker, 1995). This biosynthetic method provides a straightforward strategy for labeling any carbon on the heme molecule, provided that a suitable choice of labeled ALA is made. Heme, labeled exclusively at the heme propionate carbonyl carbons, was prepared using [1-^{13}C]ALA as a precursor in the heme biosynthesis shown schematically in Figure 1. When [3-^{13}C]ALA is used as a heme precursor, heme labeled at four β-pyrrole, two α-vinyl, and two α-propionate carbons is obtained (Figure 1A). Cytochrome b_5, as isolated from beef liver, is heterogeneous in solution as a result of heme being bound to the polypeptide in one of

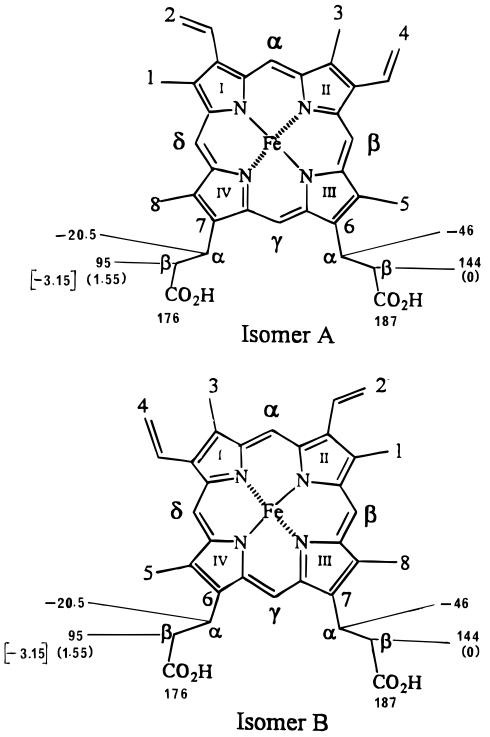

FIGURE 2: Diagram of the two heme orientations which differ by a 180° rotation about the α,γ-meso axis which results in heme disorder. The methylene carbons in the heme propionate side chains are also labeled α and β. The corresponding chemical shifts are indicated by the following: numbers = ^{13}C resonances, (numbers) = one set of diasterostopic ^{1}H resonances, and [numbers] = a second set of diasterostopic ^{1}H resonances.

two orientations related to each other by a 180° rotation about the porphyrin α,γ-meso axis, as shown in Figure 2 (Keller & Wüthrich, 1980; La Mar *et al.*, 1981), hence giving rise to heme isomers A and B. The same type of heme disorder has been observed for different forms of cytochrome b_5 expressed in bacteria (Keller & Wüthrich, 1980; Lee *et al.*, 1990), and it is noteworthy that the heme orientation ratio A:B varies from 9:1 for beef microsomal cytochrome b_5 (Wüthrich, 1980; La Mar *et al.*, 1981) to 1:1 for rat liver OM cytochrome b_5 (Rivera *et al.*, 1992). The spectroscopic consequence of the two heme orientations is the doubling of almost every ^{13}C resonance arising from the prosthetic group.

The ^{13}C NMR spectra of OM cytochrome b_5 whose heme has been enriched with ^{13}C using [3-^{13}C]ALA, [1-^{13}C]ALA, and [1,2-^{13}C]ALA are shown in Figure 3a−c, respectively. The resonances labeled A6CO and B7CO in Figure 3b arise from the heme carbonyl carbon on position 6 in isomer A and from the heme carbonyl carbon on position 7 in isomer B, respectively (see Figure 2). The strategy followed for the assignment of these resonances to their corresponding carbonyl carbons was as follows: [3-^{13}C]ALA was used as a heme precursor in order to obtain cytochrome b_5 with heme labeled at positions 6-propionate α and 7-propionate α in isomer A (A6α and A7α, respectively) and at positions B6α and B7α in isomer B. In order to assign these carbons to their corresponding resonances, an HSQC experiment (Figure 4a) was performed on this sample in order to take advantage of the already known proton chemical shifts of the hydrogens directly attached to these propionate α carbons (McLachlan *et al.*, 1986b; Rivera *et al.*, 1992). This experiment demonstrated that the ^{13}C resonances at −46 ppm arise from

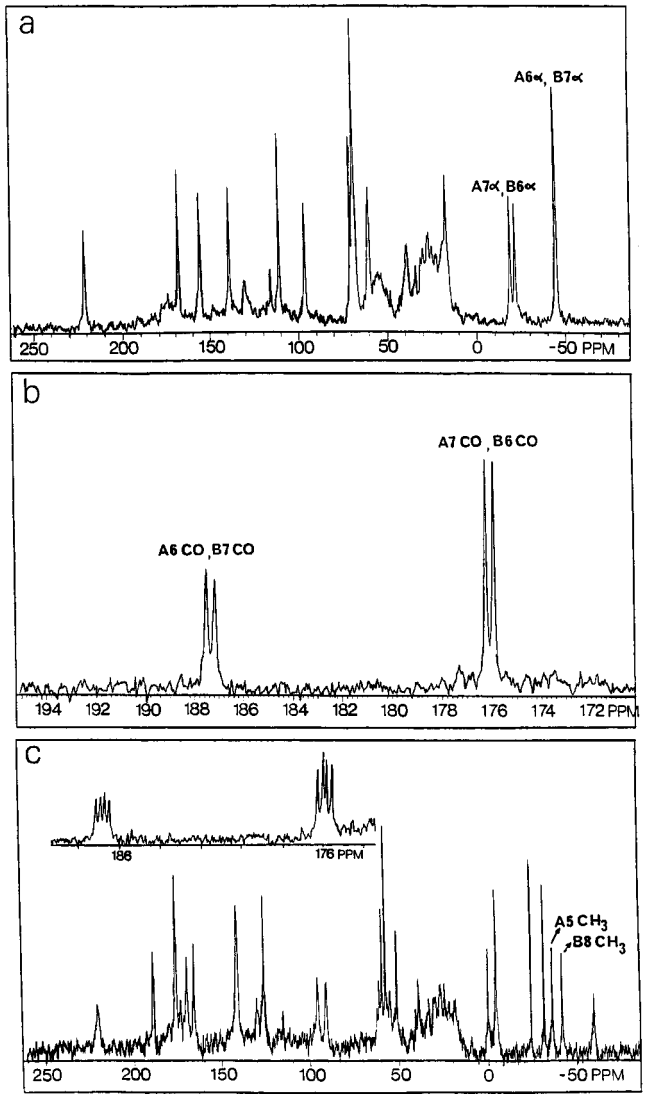

FIGURE 3: ^{13}C NMR spectra of OM cytochrome b_5 whose heme has been labeled using (a) [3-^{13}C]ALA, (b) [1-^{13}C]ALA, and (c) [1,2-^{13}C]ALA as heme precursors. The inset in spectrum c corresponds to the carbonyl region which shows ^{13}C coupling between the heme propionate β and carbonyl carbons. The chemical shift was determined using an external substitution reference consisting of dioxane in D_2O at 67.66 ppm.

carbons A6α and B7α and that the resonances centered at −20.5 ppm arise from carbons A7α and B6α (see Figure 2). The same sample was used to correlate the heme propionate α carbons with the heme propionate β hydrogens via a heteronuclear multiple-bond correlation experiment (HMBC). The results from this experiment (Figure 4b) show that the ^{13}C resonances arising from carbons A7α and B6α, centered at −20.5 ppm, have cross-peaks with protons resonating at 1.63 and 1.50 ppm, thus indicating that heme propionate β-hydrogens, A7Hβ and B6Hβ, in OM cytochrome b_5 resonate at 1.50 and 1.63 ppm, respectively. HMBC correlations between A6Hβ or B7Hβ resonances and A6α or B7α methylene carbons at −46 ppm were not observed with this experiment (see below).

The remainder of the assignments were carried out with a sample of OM cytochrome b_5 whose heme was labeled at the heme propionate carbonyl and heme propionate β carbon using [1,2-^{13}C]ALA as a heme precursor (see Figure 1B). The resultant carbonyl carbon resonances consist of two sets of signals, each consisting of two doublets, one centered at

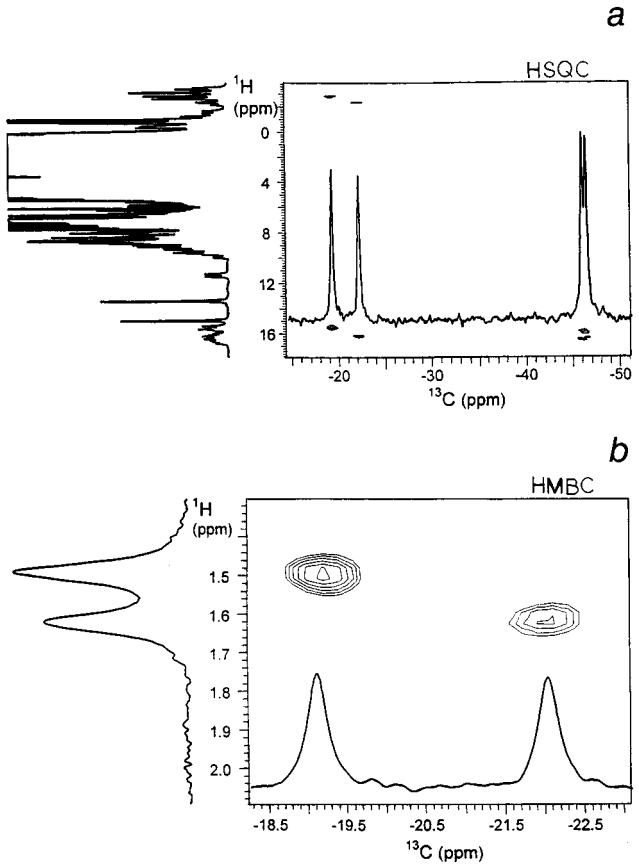

FIGURE 4: (a) Portion of the HSQC spectrum of OM cytochrome b_5 labeled with [3-^{13}C]ALA. The isotropic chemical shifts of the diasterostopic 7-α-methylene protons are very different (near 16 and −3 ppm), whereas the chemical shifts of the 6−α-methylene protons are almost identical (near 16 ppm). This observation has been explained by McLachlan *et al.* (1986a). (b) Portion of the HMBC spectrum of the same sample described above. The chemical shift references were HOD at 4.8 ppm for ^{1}H and dioxane in D_2O at 67.66 ppm for ^{13}C.

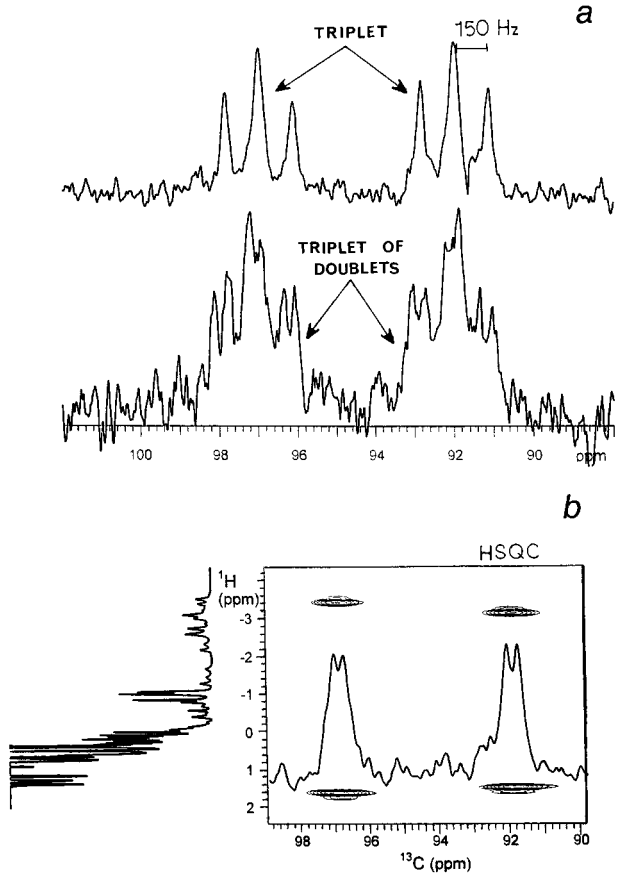

FIGURE 5: (a) ^{13}C homodecoupling experiment carried out with a sample of OM cytochrome b_5 which had been enriched using [1,2-^{13}C]ALA. (b) Portion of the HSQC spectrum obtained with a sample of OM cytochrome b_5 labeled with [1,2-^{13}C]ALA.

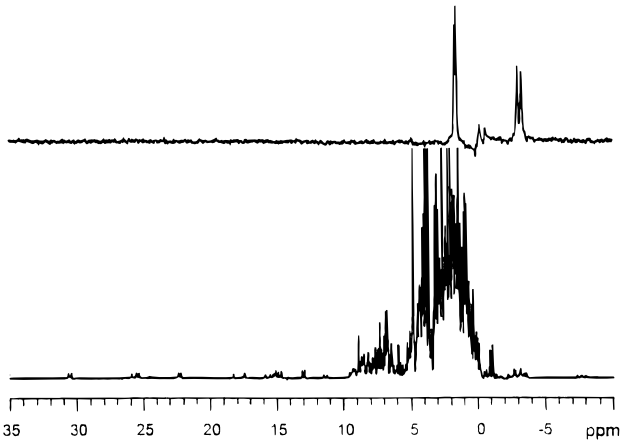

FIGURE 6: ^{13}C−^{13}C double-quantum-filtered experiment used to selectively pick out ^{13}C−^{13}C−^{1}H fragments from a large number of overlapping ^{1}H resonances: (bottom) full spectrum of OM cytochrome b_5 labeled with [1,2-^{13}C]ALA and (top) spectrum of doubly labeled fragments.

176 ppm and the second one at 187 ppm (inset of Figure 3c). The doublets arise from ^{13}C homonuclear coupling between the heme propionate β and carbonyl carbons. ^{13}C-selective homodecoupling of each set of carbonyl resonances was carried out next in order to obtain ^{13}C spectra. Irradiation of the pair of doublets centered at 176 ppm results in the collapse of the two triplets of doublets at 92 and 97 ppm into two triplets with a J_{CH} of 150 Hz (Figure 5a), thus indicating that the triplets at 92 and 97 ppm arise from methylene β carbons bound to the irradiated carbonyl carbons (one from each isomer). The resonances arising from the protons attached to these methylene β carbons at 92 and 97 ppm were assigned via an HSQC experiment (Figure 5b). The chemical shifts of these methylene β hydrogens were found to be 1.50 and 1.63 ppm. It is noteworthy that the ^{1}H resonances at 1.50 and 1.63 ppm had been previously assigned to heme propionate β hydrogens, A7Hβ and B6Hβ, with the aid of an HMBC experiment (Figure 4b), therefore demonstrating that the carbonyl resonances at 176 ppm arise from carbonyl A7CO and B6CO, which correspond to the propionate located on the buried heme edge. Consequently, the carbonyl resonances arising from the heme propionate located on the exposed heme edge, A6CO and B7CO, correspond to those centered at 187 ppm (Figure 3b).

The HSQC experiment (Figure 5b) showed an additional set of ^{1}H cross-peaks at −3.03 and −3.32 ppm in addition to the cross-peaks at 1.50 and 1.63 ppm which were also obtained from the HMBC experiment (Figure 4b). In order to corroborate the assignments described above and to investigate the nature of the peaks at −3.03 and −3.32 ppm, a ^{13}C−^{13}C double-quantum filter experiment with ^{1}H detection was used to selectively pick out ^{13}C−^{13}C−^{1}H fragments from a large number of overlapping proton resonances (Qiu *et al.*, manuscript in preparation). The results depicted in Figure 6 show that the pair of ^{1}H peaks at 1.50 and 1.63 ppm and the pair at −3.03 and −3.32 ppm correspond to

heme propionate β hydrogens A7Hβ and B6Hβ. The set of resonances at −3.03 and −3.32 ppm is broader than the set at 1.50 and 1.63 ppm, indicating a shorter T_2 and providing a probable explanation for our failure to observe them with the HMBC experiment. The broad peaks near 0 ppm in the ^{1}H−^{13}C−^{13}C experiment are linked by HSQC to A6β and B7β methylene carbons (144 ppm) and by homodecoupling to A6CO and B7CO (187 ppm) (data not shown).

NMR Titrations. ^{13}C resonances arising from the heme in OM cytochrome b_5 were used to monitor the titration of rat liver OM cytochrome b_5 with horse heart cytochrome *c*. The cytochrome b_5−cytochrome *c* complex is in fast exchange between its free and bound forms, and consequently, the shift induced on cytochrome b_5 resonances upon complexation with cytochrome *c* at any point in the titration is a weighted average of the chemical shifts corresponding to free and bound cytochrome b_5, as shown by eq 1.

$$\delta_o = \delta_b \alpha_b + \delta_{bc} \alpha_{bc} \quad (1)$$

The terms α_b and α_{bc} represent the fractions of free and complexed cytochrome b_5, respectively, and the terms δ_o, δ_b, and δ_{bc} represent the observed chemical shift at any point during the titration, the chemical shift of free cytochrome b_5, and the chemical shift of fully complexed cytochrome b_5, respectively.

The titration curve shown in Figure 7a was constructed by monitoring resonances arising from heme propionate α methylene carbons. This titration curve clearly shows that, upon addition of cytochrome *c* to a solution containing OM cytochrome b_5, the resonances arising from methylene α carbons A6α and B7α (●) shift, whereas resonances corresponding to methylene α carbons A7α and B6α (▲, ■) are not affected. The titration curve constructed from monitoring the heme propionate carbonyl carbons (Figure 7b) also shows that carbonyl carbon resonances arising from A6CO and B7CO (●, ■) in OM cytochrome b_5 are shifted as a function of cytochrome *c* concentration, whereas the carbonyl carbon resonances arising from A7CO and B6CO (▲, ▼) remain unperturbed. It can also be seen from these titration curves that the resonances are no longer perturbed upon addition of cytochrome *c* when the cytochrome *c*:cytochrome b_5 ratio is 1.25 or larger, which indicates that the complex formed between cytochrome b_5 and cytochrome *c* has 1:1 stoichiometry.

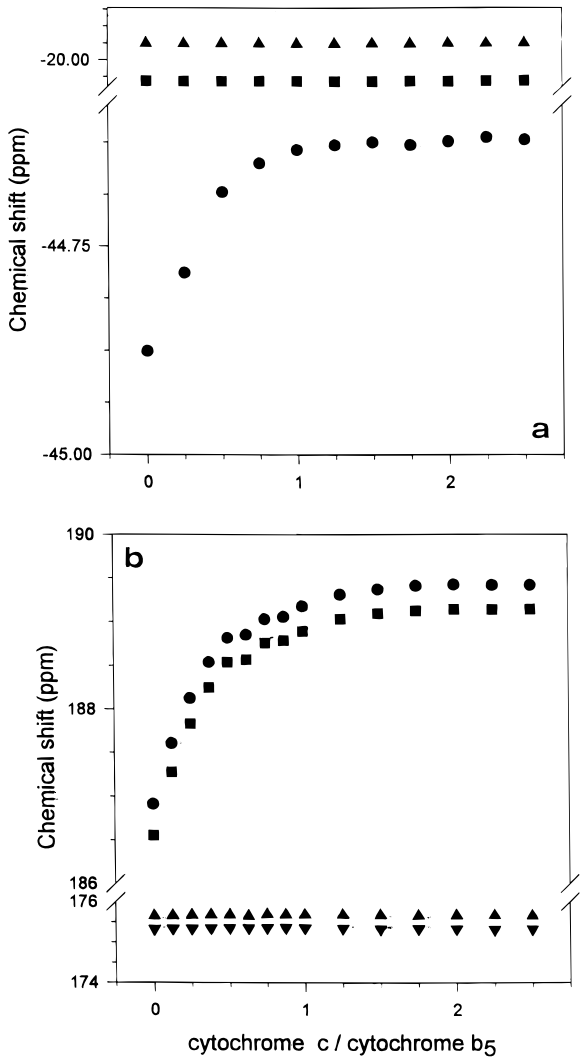

FIGURE 7: Curves for the titration of OM cytochrome b_5 with horse heart cytochrome *c*. (a) (●) Resonances arising from heme methylene α carbons A6α and B7α and (▲, ■) heme propionates A7α and B6α which are not affected. (b) (●, ■) Resonances arising from heme carbonyl carbons A6CO and B7CO and (▲, ▼) resonances arising from A7CO and B6CO.

DISCUSSION

Three-Dimensional Structure of OM Cytochrome b_5. The structural features of the water soluble domain of OM cytochrome b_5 are very similar to those reported for the water soluble domain of lipase-solubilized bovine liver cytochrome b_5 (Durley & Mathews, 1996). This is illustrated in the stereodiagram of the α carbon backbone trace of the two superimposed proteins depicted in Figure 8. The rms (root mean square) difference between the crystal structure coordinates of the backbone atoms in the two forms of cytochrome b_5 is 0.6 Å (residues 5−84). This observation is consistent with the fact that the two cytochromes b_5 have approximately 60% homology in their amino acid sequence and there are no deletions or insertions in their aligned amino acid sequences (Lederer *et al.*, 1983; Rivera *et al.*, 1992). The homology between the two crystal structures may also be, to a large extent, the reason for the successful application of molecular replacement methods in solving the phase problem for the OM cytochrome b_5 using the structure of the microsomal isoform as a search model. Since the structure of mitochondrial cytochrome b_5 was refined with 2.7 Å resolution data while the structure of microsomal cytochrome b_5 was refined using higher-resolution data (Durley & Mathews, 1996), it is relevant to compare the two crystal structures at medium resolution. The similarity of the two structures is not only confined to the C-α backbones but also extended to the side chain rotamers; *i.e.*, the difference between their side chain χ torsional angles is smaller than 60° for most amino acid residues. If the Ala, Gly, or Pro residues in the mitochondrial and microsomal amino acid sequence are excluded, only 8 out of 69 residues are observed to have different rotamers in the two crystal structures. These include Leu9, Glu11, Glu43, Glu44, Ser57 (Asn in microsomal cytochrome b_5), Val61, Leu70 (Met), and Ser71 (Leu). Some of these different rotamers can be rationalized by changes in the crystal packing (*e.g.*, residues 43 and 44), changes in the stereochemistry environment caused by surrounding amino acid substitutions in the three-dimensional structure (*e.g.*, residues 9 and 11), and changes

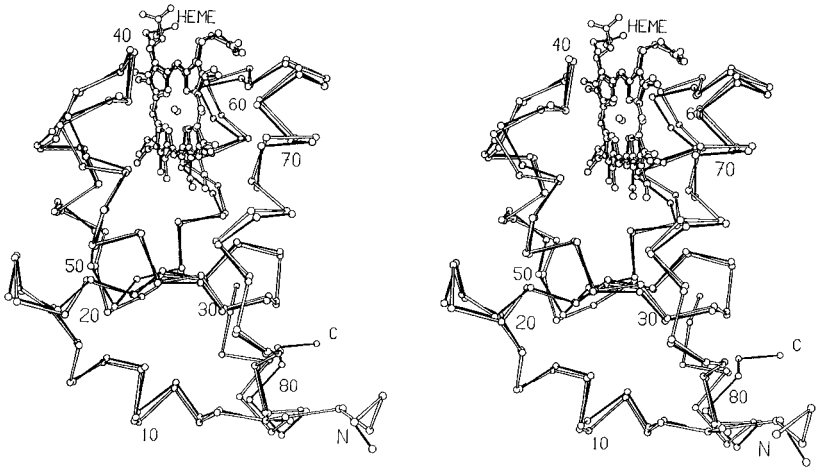

FIGURE 8: Stereodiagram of the C-α backbone superposition of the crystal structures of OM cytochrome b_5 (solid bonds) and calf liver microsomal cytochrome b_5 (open bonds). The heme groups from both crystal structures are included. The superposition of the two structures was optimized using C-α atoms of residues 5−84. The amino and carboxyl termini are labeled N and C, respectively.

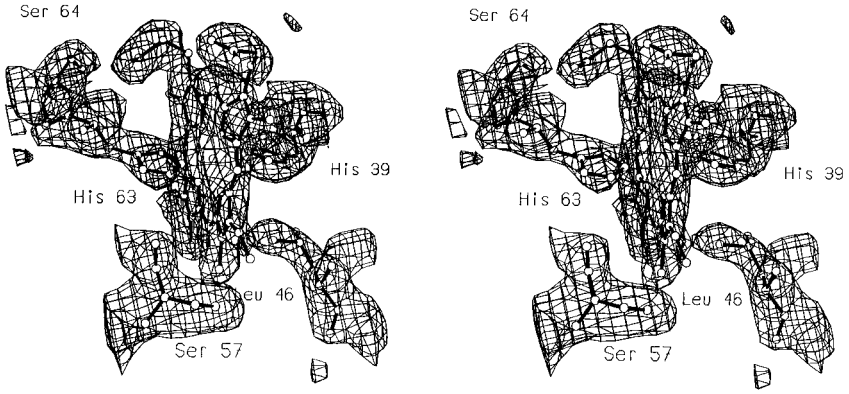

FIGURE 9: Stereoview of the heme group and some surrounding amino acid residues. The 2.7 Å ($2F_o - F_c$) electron density map is contoured at 1.0σ, where σ is the standard deviation of the map over the whole unit cell. Phases of the map are from the refined crystal structure of OM cytochrome b_5.

in hydrogen-bonding partners (*e.g.,* Ser71 to Leu substitution). The tendency to conserve side chain rotamers in homologous protein molecules has also been observed in other protein structures (Baldwin *et al.,* 1993).

The heme environment in OM cytochrome b_5 is also very similar to that observed in the microsomal isoform (Durley & Mathews, 1996). It consists of a four-α-helix bundle that surrounds the heme molecule and a three-strand β-sheet that forms the bottom of the heme pocket, leaving one edge and the top part of the heme group exposed to the aqueous environment. The heme iron in the mitochondrial protein is also octahedrally coordinated, with His39 and -63 acting as the two axial ligands. Heme propionate 7 in the mitochondrial protein forms hydrogen bonds with the Ser64 hydroxyl and amide groups as observed in the structure of microsomal cytochrome b_5; heme propionate 6 in the static structure of OM cytochrome b_5, on the other hand, adopts a conformation different from that observed in the structure of the microsomal protein. Specifically, the carbonyl carbon of heme propionate 6 is not completely exposed to the aqueous environment, and it does not form hydrogen bonds or electrostatic interactions with atoms in the protein backbone (Figure 9).

Outside of the amino and carboxy termini regions, the largest difference between the crystal structures of microsomal and mitochondrial cytochromes b_5 occurs in the region between residues 52 and 65. It is interesting to notice that there are three nonconserved residues in this region, specifically Gly52Ala, Asn57Ser, and Thr65Pro, residues in microsomal cytochrome b_5 listed first. The β-methylene group in the side chains of Asn57 and Gln49 in microsomal cytochrome b_5 are in van der Waals contact with heme 4-vinyl in isomer A, which is located on the exposed heme edge of microsomal cytochrome b_5, therefore providing a hydrophobic microenvironment to this heme substituent, while the remainder of the Asn57 and Gln49 side chains, including the hydrophilic amido groups, point away from the heme. The hydroxy group of Ser57 in OM cytochrome b_5, on the other hand, is in van der Waals contact with the heme 4-vinyl β carbon in isomer A. Moreover, the hydroxy group in Ser57 forms a hydrogen bond with the carbonyl group in Gln49, which is also in van der Waals contact with heme 4-vinyl β group, therefore providing a hydrophilic microenvironment for this heme substituent, which extends the hydrophilic environment of the exposed heme edge in OM cytochrome b_5 to include heme 4-vinyl β group in isomer A and possibly heme 1-methyl in isomer B. This may be partially responsible for the more negative (∼100 mV) reduction potential observed for OM cytochrome b_5 since this observation is in agreement with the postulated effect of solvation of the heme by the protein-aqueous environment. For example, Kassner (1972, 1973) suggested that the nonpolar environment of the heme in cytochrome *c* accounted for the fact that the reduction potential of this

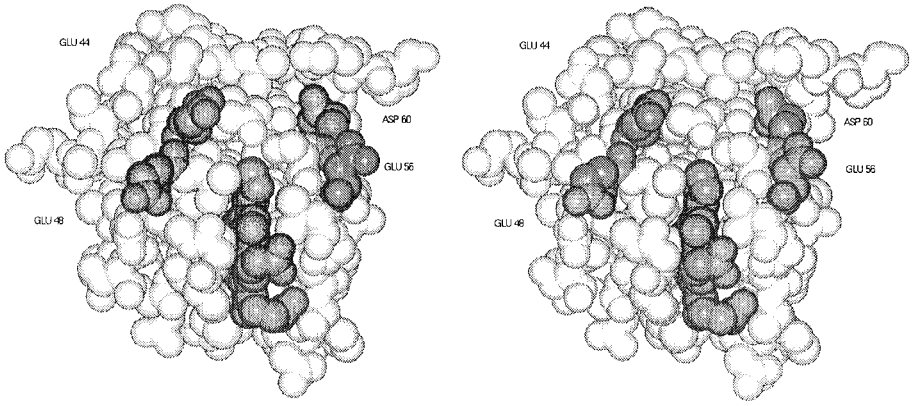

FIGURE 10: Stereoview of OM cytochrome b_5 in a space-filling diagram highlighting the heme and acidic residues Glu44, Glu48, Glu56, and Asp60. These four residues surround the exposed heme edge where heme propionate 6 in isomer A or heme propionate 7 in isomer B is located.

protein is approximately 300 mV more positive than the reduction potential of heme models of cytochrome *c*. This was later reinforced by a theoretical modeling study (Churg & Warshel, 1986) which pointed out that the major source of the 300 mV difference between the redox potential of cytochrome *c* and its octapeptide is due to the destabilization of the positive charge in the oxidized state of the heme in cytochrome *c*. Charge destabilization can be attributed to the nonpolar, low-dielectric local heme microenvironment, which results in a positive shift of the reduction potential of cytochrome *c* with respect to the heme octapeptide.

^{13}C NMR Titrations. Heme propionate A6 or B7 is located on pyrrole ring III, which is on the heme edge that is exposed to the aqueous environment, as shown in Figure 10, whereas heme propionate A7 or B6 is located on pyrrole ring IV, which is on the heme edge that is buried in the hydrophobic heme binding site. The carboxyl group of this propionate group forms a hydrogen bond to Ser64 and its carbonyl carbon is almost completely buried. When cytochrome *c* is added to a solution containing cytochrome b_5, the titration curves shown in panels a and b of Figure 7 show that shifts are observed exclusively for those resonances arising from the carbonyl carbon and methylene α carbon located on the heme propionate that is on the solvent-exposed heme edge, A6Prop or B7Prop, thus indicating that this heme propionate participates in the electrostatic binding between the two cytochromes. Those resonances attributed to the heme propionate located on the buried heme edge, A7Prop or B6Prop, on the other hand, are not influenced upon addition of cytochrome, thus strongly indicating that this heme propionate does not participate in electrostatic binding to cytochrome *c*.

These experimental observations are consistent with the model proposed for the microsomal cytochrome b_5−cytochrome *c* complex proposed by Salemme (1976), on the basis of molecular modeling, and more recently by Northrup *et al.* (1993), on the basis of Brownian dynamics calculations. The model proposed by Salemme predicted that the cytochrome b_5−cytochrome *c* complex is stabilized by electrostatic interactions between Glu44 and Lys27, Glu48 and Lys13, Asp60 and Tml72 (Tml = trimethyllysine), and heme propionate (A6Prop) and Lys79 (cytochrome b_5 residues listed first). The model obtained by Brownian dynamics calculations also predicted the participation of heme propionate A6Prop. In this model, the electrostatic interactions occur between Glu48 and Lys13, Glu56 and Lys87, Asp60 and Lys86, and A6Prop and Tml72. It is noteworthy that the Salemme model and that obtained by Brownian dynamics calculations are spatially related by a simple translation of cytochrome b_5 along the surface of cytochrome *c* (Northrup *et al.*, 1993), which has been interpreted as a corroboration of the fact that the cytochrome b_5−cytochrome *c* complex is highly dynamic. The experimental observation of the participation of the heme propionate on pyrrole ring III reported here is also in agreement with a model derived from hyperbaric UV−vis spectroscopic studies in combination with site-directed mutagenesis (Rodgers *et al.*, 1988; Sligar *et al.*, 1991), which demonstrated that the major interaction site on the surface of microsomal cytochrome b_5 is near the exposed heme edge and that this site involves acidic residues Glu44, Glu48, Glu56, and Asp60 and the heme propionate located on pyrrole ring III, as shown in Figure 10.

Stoichiometry and Stability of the OM Cytochrome b_5−Cytochrome c Complex. The shifts induced in the resonances arising from the heme propionate located on the exposed heme edge of cytochrome b_5 saturate at a cytochrome *c*:cytochrome b_5 molar ratio of approximately 1.25. This observation suggests the formation of a complex with 1:1 stoichiometry. These results are in good agreement with the stoichiometry obtained for the complex formed between microsomal cytochrome b_5 and horse heart cytochrome *c* by Mauk *et al.* (1982), using visible spectroscopy, and by Eley and Moore (1983), using ^{1}H NMR spectroscopy, and more recently by McLean and Sligar (1995), who utilized isothermal titration calorimetry to determine the stoichiometry and stability of the complex. Whitford *et al.* (1990), on the other hand, reported the possibility of a ternary complex consisting of two molecules of cytochrome *c* and one molecule of cytochrome b_5 on the basis of ^{1}H NMR experiments. These authors reported that the resonance corresponding to the propionate 6−α-methylene hydrogens in isomer A shifted first to high frequency after the addition of the first equivalent of cytochrome *c*; the same resonance shifted to low frequency upon addition of the second equivalent of cytochrome *c*. The ^{13}C heme propionate chemical shifts reported here, however, shift only to high frequency upon addition of cytochrome *c* and saturate at cytochrome *c*:cytochrome b_5 ratios greater than 1.25.

Spectral crowding in ^{1}H NMR spectra of mixtures containing cytochrome b_5 and cytochrome *c* makes the titration experiments relatively difficult to interpret, and this situation is exacerbated by virtual doubling of all paramag-

netically shifted resonances arising from OM cytochrome b_5 heme isomers which are present in solution with equal concentrations (Rivera *et al.*, 1992). The spectral crowding observed in the ^{1}H NMR spectra of mixtures of cytochrome *c* and cytochrome b_5 is overcome by observing ^{13}C NMR resonances arising from ^{13}C-enriched heme cytochrome b_5. These experiments clearly show the formation of a cytochrome b_5−cytochrome *c* complex with 1:1 stoichiometry. An additional advantage is gained by observing the resonances arising from the carbonyl carbons throughout the titration. These resonances are minimally affected by the unpaired electron in the heme iron, as demonstrated by their relatively narrow line widths (∼10 Hz) and by their chemical shifts which are in good agreement with chemical shifts observed for carbonyl carbons in diamagnetic compounds.

The value for the conditional binding constant for the equilibrium shown in eq 2 was obtained from the NMR titration data as described below:

$$b_5 + c \rightleftarrows b_5c \quad K = \frac{[b_5c]}{[b_5][c]} \tag{2}$$

$$A_b = [b_5] + [b_5c] \tag{3}$$

$$A_c = [c] + [b_5c] \tag{4}$$

Equations 3 and 4 represent the mass balance for the equilibrium shown in eq 2. The terms $[b_5]$, $[c]$, and $[b_5c]$ represent the concentrations of free cytochrome b_5, free cytochrome *c*, and the complex, respectively. The terms A_b and A_c represent the analytical concentration of cytochrome b_5 and cytochrome *c*, respectively. The concentration of free cytochrome *c* at any point in the titration curve can be expressed as a function of the analytical concentrations of cytochrome b_5, cytochrome *c*, and the binding constant, *K*, by combining eqs 2−4 to obtain eq 5.

$$[c] = \frac{A_c - [c]}{K(A_b - A_c + [c])} \tag{5}$$

If the mole fraction terms α_a and α_{bc} in eq 1 are expressed according to eqs 6 and 7, and subsequently combined with eq 1 and the equilibrium expression, an equation that relates the experimentally observed chemical shift at any point in the titration curve to the corresponding concentration of free cytochrome *c* is readily obtained (eq 8). The constants δ_b and δ_{bc} represent the chemical shift of OM cytochrome b_5 in its free and fully complexed states, respectively. The value of δ_b was obtained from a solution containing only cytochrome b_5, and the value of δ_{bc} is obtained in the presence of a large excess of cytochrome *c*, in this case the last point in the titration curve.

$$\alpha_b = \frac{[b_5]}{[b_5] + [b_5c]} \tag{6}$$

$$\alpha_{bc} = \frac{[b_5c]}{[b_5] + [b_5c]} \tag{7}$$

$$\delta_o = \frac{\delta_b - \delta_{bc}}{1 + K[c]} + \delta_{bc} \tag{8}$$

A binding curve was constructed by first calculating the concentration of free cytochrome *c* at any point in the titration curve utilizing eq 5. To this end, the binding constant *K* was initially assumed to have a value of 1.0×10^3 M^{-1}. The calculated values of $[c]$ and the assumed value of *K* were subsequently used to calculate the value of the observed chemical shift (δ_o) at any point in the titration curve by substituting these values in eq 8. If the agreement between experimental and calculated binding curves was not acceptable, the process was started again with a more suitable value of the binding constant *K*. Binding curves were constructed in this manner for those resonances that are in a relatively uncrowded region of the ^{13}C spectrum and whose chemical shifts are perturbed upon addition of titrant (cytochrome *c*). The results are summarized in Figure 11 which shows fitted and experimental binding curves for ^{13}C resonances arising from the following heme substituents: (a) heme propionate A6α and B7α, (b) B 4-vinyl α, (c) A 5-methyl, and (d) B 8-methyl. The value of the conditional binding constant for the formation of the OM cytochrome b_5−cytochrome *c* complex at $\mu = 0.02$ M and $T = 30$ °C is $3.8 \times 10^4 \pm 1.4 \times 10^4$ M^{-1}. Eley and Moore (1983) reported a value of 960 ± 100 M^{-1} at $\mu = 0.04$ M for the formation of the complex between microsomal cytochrome b_5 and cytochrome *c*, obtained using ^{1}H NMR spectroscopy. These investigators calculated the value of the binding constant with an equation that is valid only under conditions where the fraction of cytochrome b_5 bound is negligible compared with the fraction unbound. The binding curves obtained at $\mu = 0.02$ M (Figure 11) show rapid saturation of the cytochrome b_5 chemical shifts upon addition of cytochrome *c*, which is consistent with the higher stability of the complex at the lower ionic strength used in the experiments reported here, and it is therefore not possible to assume that the fraction of bound cytochrome *c* is negligible compared with the fraction unbound. For example, if a low value of the binding constant is assumed, which corresponds to a negligible fraction of bound cytochrome *c*, the observed chemical shift does not saturate in the explored range of concentrations, as shown in Figure 12a. On the other hand, when *K* is allowed to take progressively larger values, the chemical shift saturates at progressively lower concentrations of titrant.

Attempts to construct a binding curve with chemical shifts that arise from the heme propionate carbonyl located on the exposed side of the heme resulted in curves displaying a different behavior. The experimental binding curve (▲ in Figure 12b) displays chemical shifts that are substantially larger than those calculated from eq 8 even when the assumed value of the binding constant is relatively large. Close inspection of this binding curve reveals that in the initial stages of the titration, when the concentration of cytochrome *c* is relatively low compared to that of cytochrome b_5, the induced chemical shifts are larger than those predicted by the model. This suggests that, if the ionic strength remained constant throughout the titration, the value at which the chemical shift saturates must be larger than is observed experimentally. This can be explained by invoking the fact that the ionic strength of the solution increases upon addition of cytochrome *c* and that the carbonyl carbon chemical shifts are largely susceptible to ionic interactions between the heme propionate in cytochrome b_5 and lysyl groups in cytochrome *c*. In the titration experiments reported here, the ionic strength starts at 0.01 M and it increases to approximately 0.02 M after addition of 1 equiv of cytochrome *c*; thus, it is likely that in the initial stages of the titration, when the ionic

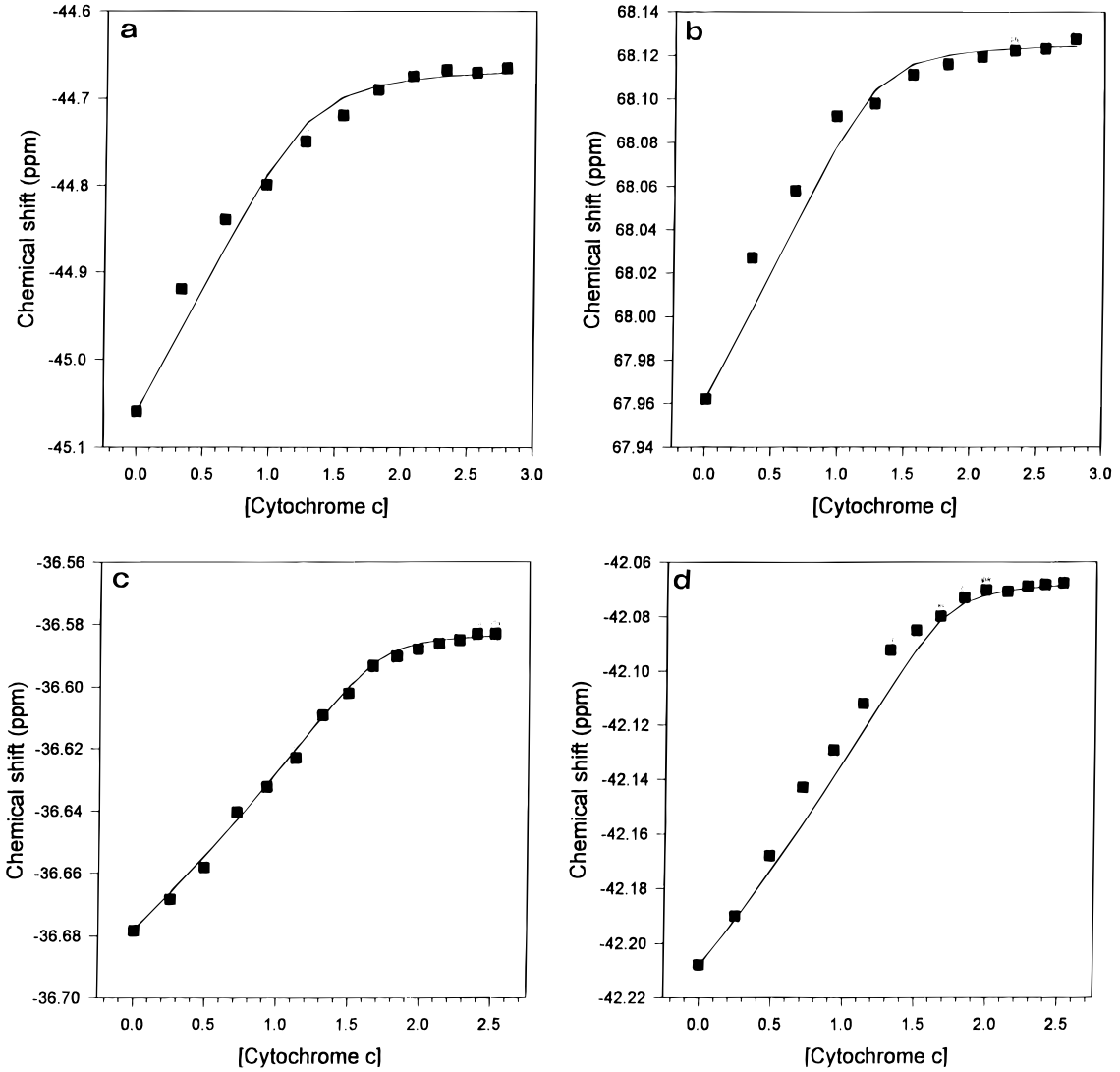

FIGURE 11: Experimental (■) and fitted (—) binding curves constructed for the evaluation of the binding constant K by monitoring (a) ^{13}C resonance arising from A6α or B7α carbon ($K = 2.2 \times 10^4$ M^{-1}), (b) ^{13}C resonance arising from B-4-vinyl α carbon ($K = 3.0 \times 10^4$ M^{-1}), (c) ^{13}C resonance arising from A-5 Me carbon ($K = 5.0 \times 10^4$ M^{-1}), and (d) ^{13}C resonance arising from B-8 Me carbon ($K = 5.0 \times 10^4$ M^{-1}). The value for K of $3.8 \times 10^4 \pm 1.4 \times 10^4$ M^{-1} reported in the text is an average of the values above.

strength is relatively low, electrostatic interactions are stronger, therefore resulting in relatively large initial shifts of the carbonyl resonances. Presumably, if the ionic strength of the solution did not change throughout the titration, the saturation of the carbonyl chemical shift would occur at a larger value, as shown by the dashed line in Figure 12b. The sensitivity of ionic interactions to the ionic strength of the solution therefore renders the carbonyl chemical shifts inappropriate for the calculation of the binding constant. It is important to stress, however, that the selective shifts of resonances arising from these carbonyls allow the experimental confirmation of the role played by the heme propionate located on the exposed heme edge of cytochrome b_5 in its electrostatic binding to cytochrome *c*.

The Coulombic forces necessary for the interaction between the two cytochromes must have a large negative ionic strength dependence, as demonstrated experimentally by Mauk *et al.* (1982). The ionic strength dependence of the binding constant for the microsomal cytochrome b_5—cytochrome *c* complex is depicted in Figure 13, where ● and ▲ correspond to the values of the binding constant obtained by Mauk *et al.* (1982) utilizing visible spectroscopy and by Eley and Moore (1983) using ^1H NMR spectroscopy, respectively. The binding constant for the association between OM cytochrome b_5 and cytochrome *c* (■) shows that the stability of the complex formed by mitochondrial cytochrome b_5 and cytochrome *c* falls close to the extrapolated values obtained for the association between microsomal cytochrome b_5 and cytochrome *c*, thus indicating that the stability of the complex formed between mitochondrial cytochrome b_5 and cytochrome *c* is similar to that measured for microsomal cytochrome b_5 and cytochrome *c*.

Concluding Remarks. The three-dimensional structure of rat liver outer mitochondrial membrane cytochrome b_5 has been found to be homologous to the structure of bovine liver microsomal cytochrome b_5 (Durley & Mathews, 1996), when the structures of both proteins are compared at medium resolution. It is interesting that, despite the fact that the structure of both cytochromes b_5 is almost identical, the reduction potential of the mitochondrial protein is −102 mV *vs* NHE (Rivera *et al.*, 1994), whereas the reduction potential of the microsomal protein obtained under identical conditions of pH and ionic strength is 5.1 mV (Reid *et al.*, 1982) or −1.9 mV (Walker *et al.*, 1988). These results combined indicate that relatively large modulation of the reduction potential of bis-His-ligated heme proteins is achieved by

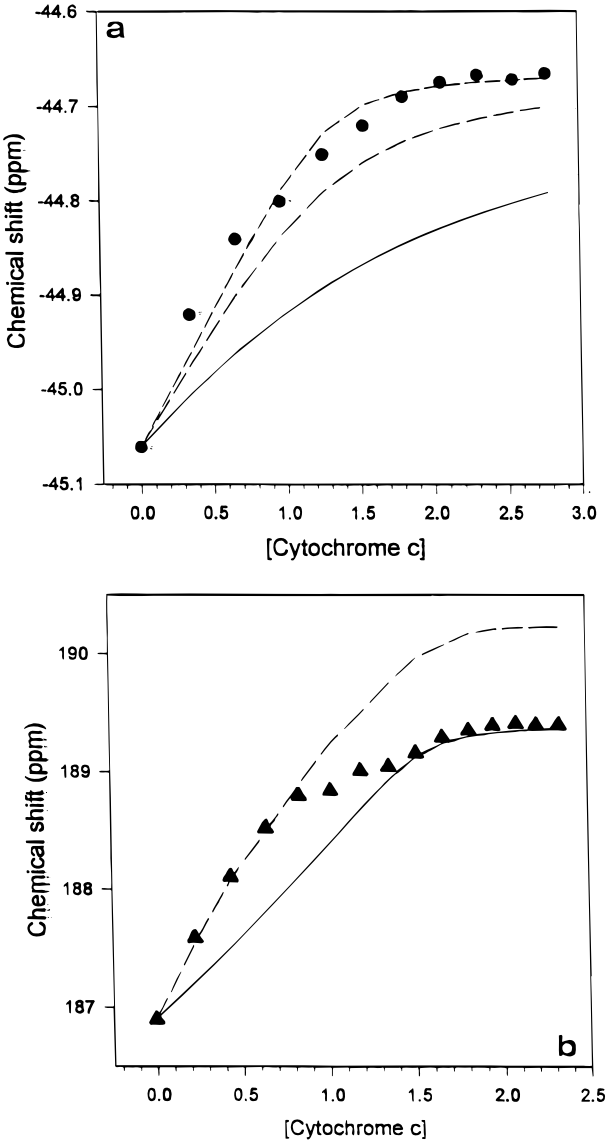

FIGURE 12: (a) Calculated binding curves constructed as a function of *K*: (—) $K = 1.0 \times 10^3$ M^{-1}, (− −) $K = 5.0 \times 10^3$ M^{-1}, and (- - -) $K = 2.2 \times 10^4$ M^{-1} (●, experimental data). (b) Experimental binding curve (▲) obtained by monitoring heme propionate carbonyl resonances. The solid line corresponds to a binding curve constructed with a *K* of 5.0×10^4 M^{-1}, while the dashed line was included to indicate that the chemical shift may saturate at a larger value if the ionic strength of the solution remained constant.

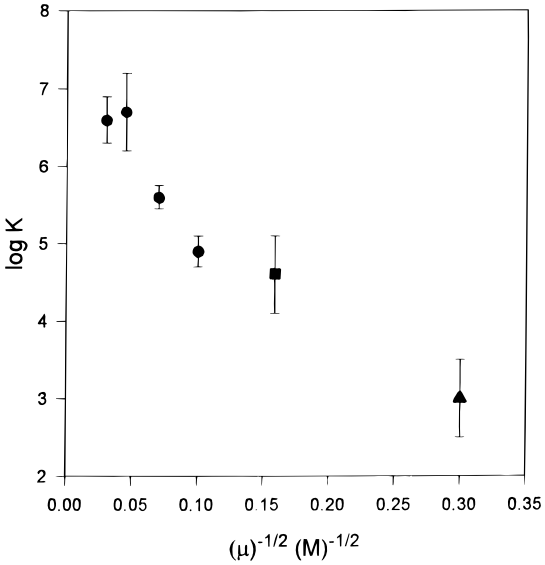

FIGURE 13: Dependence of the value of *K* on ionic strength. (●) Values obtained by Mauk *et al.* (1982) and (▲) Eley and Moore (1983) for the microsomal cytochrome b_5−cytochrome *c* complex. (■) Average value of *K* obtained from this work for the OM cytochrome b_5−cytochrome *c* complex.

subtle changes in structure. This has been documented for cytochrome *c* by Brayer *et al.* (1988), who examined the role of the invariant residue Phe82 in yeast cytochrome *c* and concluded that this residue is key in preserving the structural identity of the heme binding site by limiting solvent accessibility to the heme, thereby regulating the reduction potential of this protein dielectrically. Mutation of Phe82 to Ser resulted in the formation of a water cavity which was postulated to significantly alter the dielectric constant within the heme, thus leading to the −50 mV shift in reduction potential observed experimentally. In the structure of OM cytochrome b_5, the hydroxyl group Ser57 (Asn in microsomal cytochrome b_5) forms a hydrogen bond with the carbonyl oxygen of Glu49. Both hydrophilic groups are in van der Waals contact with heme 4-vinyl, thus providing a hydrophilic microenvironment to this heme substituent, as compared to the more hydrophobic microenvironment of the same heme substituent in microsomal cytochrome b_5. This factor may be partially responsible for the more negative reduction potential observed for OM cytochrome b_5. This hypothesis is currently under investigation in our laboratories.

The role played by the heme propionates in OM cytochrome b_5 in its electrostatic binding to cytochrome *c* was demonstrated experimentally using ^{13}C NMR spectroscopy. It is important to point out that the heme propionate carbonyl resonances are minimally affected by the unpaired electron from the heme iron, as indicated by the relatively narrow line widths of these resonances, as well as by the position of their chemical shifts which are in good agreement with chemical shifts observed for carbonyl carbons in diamagnetic molecules. The chemical shift induced in the carbonyl resonances of cytochrome b_5 upon addition of cytochrome *c*, therefore, is mainly due to electrostatic interactions formed with lysine groups in cytochrome *c* and is minimally affected by contact and dipolar interactions with the unpaired electron. Consequently, structural implications such as the exclusive participation of the heme propionate located on the exposed heme edge of cytochrome b_5 in its binding to cytochrome *c* can be readily extracted from titration experiments where the ^{13}C-enriched heme propionate carbonyl carbons in cytochrome b_5 are monitored as a function of cytochrome *c*. These NMR spectroscopic and X-ray crystallographic findings imply that the site of interaction on the surface of OM cytochrome b_5 encompasses the exposed heme edge, as previously postulated for microsomal cytochrome b_5 on the basis of computer models (Salemme, 1976; Northrup *et al.*, 1993) and hyperbaric pressure spectroscopy combined with site-directed mutagenesis (Rodgers & Sligar, 1991).

The binding constants for the cytochrome b_5−cytochrome *c* complex reported here are conditional in nature because the ionic strength of the solution changes throughout the titration due to the addition of cytochrome *c*. This is inevitable due to the relatively large concentrations needed for obtaining NMR spectra in relatively short periods of time. The conditional binding constants reported here fall close to the extrapolated line obtained by plotting the dependency of the binding constant for the complex formed by microso-

mal cytochrome b_5 and cytochrome *c* (Mauk *et al.*, 1982; Eley & Moore, 1983) on the ionic strength of the solution. This is yet another indication that the large body of information obtained for the nonphysiological system consisting of microsomal cytochrome b_5 and cytochrome *c* can be readily extrapolated to the interactions between mitochondrial cytochromes b_5 and c.

REFERENCES

Baldwin, E. P., Hajiseyedjavadi, O., Baase, W. A., & Matthews, B. W. (1993) *Science 262*, 1715−1718.

Bernardi, P., & Azzone, G. F. (1981) *J. Biol. Chem. 256*, 7187−7192.

Bodman, S. B. V., Schuller, M. A., Jollie, D. R., & Sligar, S. G. (1986) *Proc. Natl. Acad. Sci. U.S.A. 83*, 9443−9447.

Churg, A. K., & Warshel, A. (1986) *Biochemistry 25*, 1675−1681.

Durham, B., Fairris, J. L., McLean, M., Millet, F., Scott, J. R., Sligar, S. G., & Willie, A. (1995) *J. Bioenerg. Biomembr. 27*, 331−340.

Durley, R. C. E., & Mathews, F. S. (1996) *Acta Crystallogr. D52*, 65−72.

Eley, C. G. S., & Moore, G. R. (1983) *Biochem. J. 215*, 11−21.

Fukushima, K., & Sato, R. (1972) *J. Biochem. (Tokyo) 74*, 161−173.

Jones, T. A., Zou, J. Y., Cowan, S. W., & Kjeldgaard, M. (1991) *Acta Crystallogr. A47*, 110−119.

Kassner, R. J. (1972) *Proc. Natl. Acad. Sci. U.S.A. 69*, 2263−2267.

Kassner, R. J. (1973) *J. Am. Chem. Soc. 95*, 2674−2677.

Kay, L. E., Keifer, P., & Saarinen, T. (1992) *J. Am. Chem. Soc. 114*, 10663−10665.

Keller, R. M., & Wüthrich, K. (1980) *Biochim. Biophys. Acta 621*, 204−217.

Kupĉe, E., & Freeman, R. (1995) *J. Magn. Reson. 115A*, 273−276.

Kurumaya, K., Okazaki, T., Seido, N., Akasaka, Y., Kawajiri, Y., & Kajiwara, M. (1988) *J. Labelled Compds. Radiopharm. 27*, 217−235.

La Mar, G. N., Burns, P. D., Jackson, J. T., Smith, K. M., Langry, K. C., & Strittmatter, P. (1981) *J. Biol. Chem. 256*, 6075−6079.

Lederer, F., Ghrir, R., Guiard, B., Cortial, S., & Ito, A. (1983) *Eur. J. Biochem. 132*, 95−102.

Lee, B., & Richards, F. M. (1971) *J. Mol. Biol. 55*, 379−400.

Lee, K. B., La Mar, G. N., Kehres, L. A., Fujinari, E. M., Smith, K. M., Pochapsky, T. C., & Sligar, S. G. (1990) *Biochemistry 29*, 9623−9631.

Margoliash, E., & Walaseck, O. F. (1967) *Methods Enzymol. 10*, 339−348.

Matthews, B. W. (1968) *J. Mol. Biol. 33*, 491−497.

Mauk, A. G., Mauk, M. R., Moore, G. R., & Northrup, S. H. (1995) *J. Bioenerg. Biomembr. 27*, 311−330.

Mauk, M. R., Reid, L. S., & Mauk, A. G. (1982) *Biochemistry 21*, 1843−1846.

McLachlan, S. J., La Mar, G. N., & Sletten, E. (1986a) *J. Am. Chem. Soc. 108*, 1285−1291.

McLachlan, S. J., La Mar, G. N., Burns, P. D., Smith, K. M., & Langry, K. C. (1986b) *Biochim. Biophys. Acta 874*, 274−284.

McLean, M. A., & Sligar, S. G. (1995) *Biochem. Biophys. Res. Commun. 215*, 316−320.

Nisimoto, Y., Takeuchi, F., & Shibata, Y. (1977) *J. Biochem. (Tokyo) 82*, 1257−1266.

Northrup, S. H., Thomasson, K. A., Miller, C. M., Barker, P. D., Eltis, L. D., Guillemette, J. G., Inglis, S. C., & Mauk, A. G. (1993) *Biochemistry 32*, 6613−6623.

Ouwen, Z., Kay, L. E., Olivier, J. P., & Forman-Kay, J. D. (1994) *J. Biomol. NMR 4*, 845−858.

Raw, I., Petragnani, N., & Camargo-Nogueira, O. (1960) *J. Biol. Chem. 235*, 1517−1520.

Reid, L. S., Taniguchi, V. T., Gray, H. B., & Mauk, A. G. (1982) *J. Am. Chem. Soc. 104*, 7516−7519.

Rivera, M., & Walker, F. A. (1995) *Anal. Biochem. 230*, 295−302.

Rivera, M., Barillas-Mury, C., Christensen, K. A., Little, J. W., Wells, M. A., & Walker, F. A. (1992) *Biochemistry 31*, 12233−12240.

Rivera, M., Wells, M. A., & Walker, F. A. (1994) *Biochemistry 33*, 2161−2170.

Rodgers, K. K., & Sligar, S. G. (1991) *J. Mol. Biol. 221*, 1453−1460.

Rodgers, K. K., Pochapsky, T. C., & Sligar, S. G. (1988) *Science 240*, 1657−1659.

Rossmann, M. G. (1972) in *The Molecular Replacement Method*, Gordon and Breach, New York.

Salemme, F. R. (1976) *J. Mol. Biol. 102*, 563−568.

Sambrook, J., Fritsh, E. F., & Maniatis, T. (1989) in *Molecular Cloning: A Laboratory Manual*, 2nd ed., Cold Spring Harbor Laboratory Press, Plainview, NY.

Sottocasa, G. L., Kuylenstierna, B., Ernster, L., & Bergstrand, A. (1967) *J. Cell Biol. 32*, 415−438.

Stanier, R., Palleroni, N., & Dourdoroff, M. (1966) *J. Gen. Microbiol. 43*, 159−271.

Strittmatter, P., & Ozols, J. (1966) *J. Mol. Biol. Chem. 211*, 4787−4792.

Tronrud, D. E. (1996) *J. Appl. Crystallogr. 29*, 100−104.

Tronrud, D. E., Ten Eyck, L. F., & Matthews, B. W. (1987) *Acta Crystallogr. A43*, 489−503.

Walker, F. A., Emrick, D., Rivera, J. E., Hanquet, B. J., & Buttlaire, D. H. (1988) *J. Am. Chem. Soc. 110*, 6234−6240.

Whitford, D., Concar, D. W., Veitch, N. C., & Williams, R. J. P. (1990) *Eur. J. Biochem. 192*, 715−721.

Zhang, X., & Matthews, B. W. (1994) *Acta Crystallogr. D50*, 675−686.

Zhang, X., & Matthews, B. W. (1995) *J. Appl. Crystallogr. 28*, 624−630.

BI961895O